*Indian J. Met. Hydrol. Geophys.*(1977), 28, 1, 39-50

551.524 (545.5)

# Sodar studies of the thermal structure of the lower troposphere at Delhi

S. P. SINGAL, S. K. AGGARWAL and B. S. GERA

*National Physical Laboratory, New Delhi*

(*Received 15 May 1976*)

ABSTRACT. The monostatic sodar system set up at National Physical Laboratory has been operating continuously to study the thermal structure of the lower troposphere upto a vertical height of 350 m. The results obtained from December 1974 through April 1975 are presented. The observed structures showing thermal plumes, inversions, instabilities, turbulences etc developing in the atmosphere as a function of space and time have been indexed to indicate the type of meteorological conditions expected for any one of these indices.

To examine if the sodar can be used for 24 hours monitoring of atmospheric refractivity gradients, the intensity of the received echo signal at a fixed height of 150 m has been measured using a microphotometer and compared with the refractivity gradient number obtained from radiosonde data. The results show that the two techniques have a good correlation within the limits of the experimental error. These relative values of received intensity have also been used to calculate thermal structure function $C_T$. The computed values of $C_T$ have been found to compare well with Panofsky observations, showing thereby the utility of the sodar echograms to derive information of the atmospheric turbulence parameter.

## 1. Introduction

Acoustic sounding (sodar) is one of the remote sensing techniques that can give continuous information about some of the major micro-meteorological parameters of the lower atmosphere upto a height of a kilometre. Sodar essentially locates and measures the intensity of thermal and velocity inhomogeneities in the atmosphere, an information which can be used to infer and determine atmospheric processes and history. The technique can be used under clear cloudy and foggy weather and as such is useful for tropospheric communication, aviation hazards, air pollution alerts and boundary layer micrometeorological studies.

A pulsed narrow beam of sound waves is transmitted into the atmosphere where it encounters atmospheric inhomogeneities and suffers partial reflection. The reflected waves are received either by the same transducer (monostatic) or by one or more other transducers (bistatic and multistatic). The delay time and intensity are measured with each scan in the form of intensity modulation on a sweep recorder of the fascimile type displaying height range *versus* time pictures, while the shift in the carrier frequency is detected by a suitable Doppler system.

A monostatic sodar system (Singal *et al.* 1975 a) has been set up at the National Physical Laboratory with the schematic block diagram shown in Fig. 1. The reflector horn (Singal *et al.* 1975 b) has been used as the transmit-receive acoustic antenna which is a combination of a conical horn with a sector of a paraboloid of revolution such that the apex of the horn coincides with the focal point of the par aboloidal reflector. This antenna offers a 90° side lobe suppression level of 40-50 dB at a frequency of 1000 Hz and has a receiving sensitivity of 20 mV/microbar. The side lobe rejection has been further increased by surrounding the antenna with an acoustically absorbing screen (Fig. 2) designed in the shape of a regular nonagon of diagonal 3·6 metres. This acoustic screen offers an additional 90° suppression level of about 10-15 dB at the aperture of the acoustic antenna and allows the antenna to receive or transmit acoustic waves within an angle of $\pm 45°$ around the central axis. The transmit and receive circuits connected to the antenna are isolated from each other by a network of diodes as shown in the schematic. Additionally the receive circuit is blanked for the first 250 m secs to save it from the powerful transmit signal leaking to the receive circuit. The receiver pre-amplifier has a sensitivity of a fraction of a

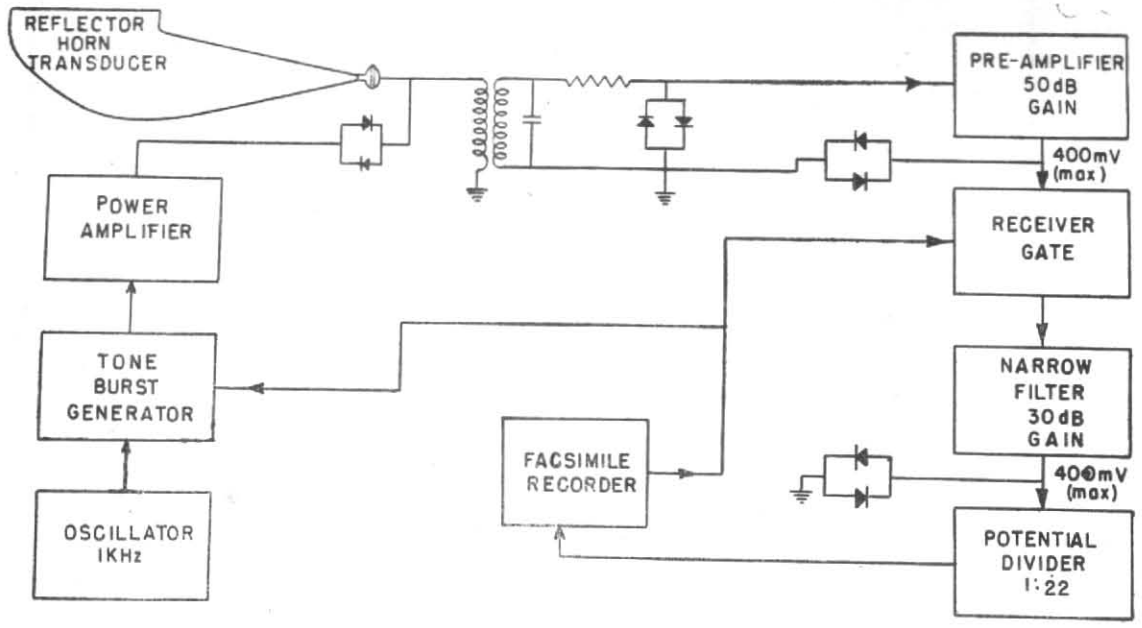


Fig. 1. Schematic block diagram of the acoustic sounder (Sodar)

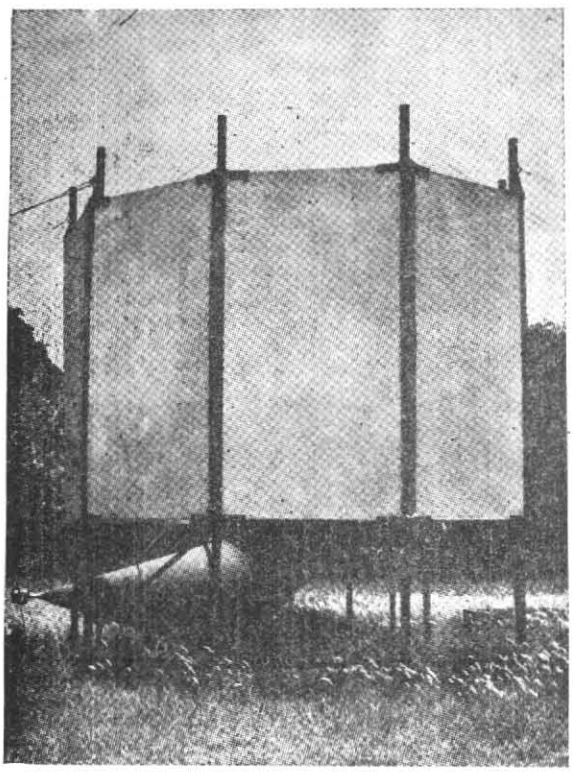

Fig. 2. Reflector horn acoustic antenna and the acoustic shield surrounding it

micro-volt. The mechanical trigger from the fascimile recorder serves as the master control centre of the system.

The system has the capability to probe the thermal structure of the lower atmosphere upto a vertical height of 350 metres which has been now extended upto 600 metres. The characteristics of this system are summarised in Table 1 which offer a range resolution of 10 metres.

Sodar experiments are being conducted at the National Physical Laboratory since 1972. The preliminary experiments (Singal and Pancholy 1972) were conducted using a collocated sounder system consisting of a cross-array of nine loudspeakers as a transmitting antenna and a paraboloid bowl with a dynamic microphone at its focus as a receiving antenna. The received signals were recorded on a photographic film from the C-scan display of an oscilloscope. Later on, the transmitting antenna was replaced by a square array of 64 cone loudspeakers and the receiving antenna was replaced by the reflector horn antenna. Mufax fascimile recorder (Singal *et al.* 1975 c) was used as the receiver in place of the photographic film. The collocated system gave place to the monostatic system described above. The extent of data obtained with the various set-ups is given in Table 2. Most of these data have been taken in the process of laying down the technique.

**TABLE 1**
**Characteristics of NPL sodar system**

| | |
|---|---|
| Transmitted power electrical | 40 watt |
| acoustical | 10 watt |
| Pulse width | 60 m sec |
| Pulse repetition rate | 0·5-0·3 pulse per sec |
| Maximum range | 600 metres |
| Receiver band width | 10-100 Hz at 1 KHz |
| Frequency of operation | 1 KHz |
| Acoustic pulse velocity | 340 m/sec (average) |
| Ambient temperature | 300 K (average) |
| Transmit/Receive transducer | Horn Reflector |
| Receiver area | 1·17 sq. m |
| Receiver sensitivity | 20 mV/$\mu$ bar (—34 dB ref. 1V/$\mu$ bar) |
| Half-width of the main lobe | $\pm$ 7 deg. |
| Recorder | Facsimile recorder |

In the following are presented the salient features of the results obtained from December 1974 through April 1975 in relation to atmospheric processes and radio communication. We also present a classification of the observed results into a number of distinct groups which will help to correlate the meteorology of the lower atmosphere with hazardous situations in communication, aviation and air pollution.

### 2. Theory

The scattering of sound waves from random fluctuations of atmospheric temperature and wind velocity within a turbulent region has been treated by Kallistratova (1961), Tatarski (1961) and Monin (1962). Applying the Kolomgorov spectrum of turbulence, the scattering cross-section as a function of scatter angle $\theta$ is given as

$$\sigma(\theta) = 0.033\, k^{1/3} \cos^2\theta \left( \frac{C_v^2}{C^2} \cos^2 \frac{\theta}{2} + 0.13 \frac{C_T^2}{T^2} \right) \left( \sin \frac{\theta}{2} \right)^{-11/3}$$

(MKS K° unit)

where $\sigma(\theta)$ is the scattered power per unit volume per unit incident flux, per unit solid angle $\theta$ being measured from the initial direction of propagation; $k = 2\pi/\lambda$ is the wave number of the acoustic wave ; $C$ and $T$ are the mean velocity of sound and mean absolute temperature of the scattering volume; and $C_v^2$ and $C_T^2$ are the structure constants for wind and temperature fluctuations respectively. The values of the two atmospheric structure constants are obtained from the following relations :

$$\overline{[u(x) - u(x+r)]^2} = C_v^2\, r^{2/3}$$

$$\overline{[t(x) - t(x+r)]^2} = C_T^2\, r^{2/3}$$

where $u$ and $t$ are wind speed and temperature respectively at a place distant $x$ and $r$ is the distance measured from the place $x$ along the x-axis.

The above expression for scattering cross section is valid only when the effective wave-number $2k \sin(\theta/2)$ lies within the inertial subrange of locally homogenous and isotropic field of wind and temperature fluctuations. Further for vertical sounding (scattering angle $\theta = 180°$), it is seen that scattering cross-section is exclusively a function of thermal structure offering a simple method of studying the temperature inhomogeneities in the lower atmosphere. The expression in this case becomes :

$$\sigma = 0.0039 \left( \frac{2\pi}{\lambda} \right)^{1/3} \left( \frac{C_T}{T} \right)^2$$

The received power $P_r$ for the vertical sounding can be estimated by following the sodar equation. It is a function of the transmitter power $P_t$ and the scattering cross section $\sigma$ for any range $R$ and can be written as :

$$P_r = n_t\, n_r\, P_t\, \sigma\, \frac{C\tau}{2}\, A_r\, \frac{1}{R^2}\, L$$

where $n_t$, $n_r$ are the transmitting and receiving efficiencies of the acoustic transducer, $\tau$ is the pulse length ; $A_r$ is the collecting area of the antenna and $L$ is the attenuation factor due to atmospheric absorption along the double path to the scattering region.

### 3. Results and discussion

In a monostatic system sodar echograms give height range *versus* time pictures displaying the intensity of back-scattered signals as indications of the strength of thermal instabilities in the lower atmosphere with the region of strong echo returns representing strata of enhanced temperature inhomogeneities. The acoustic sounder is unable to receive any echo returns from regions where temperature fluctuations are rather weak or the lapse rate of temperature is nearly adiabatic. Continuous monitoring of the lower atmosphere with sodar provides, thus, complete information about the thermal structure of the planetary boundary layer.

#### 3.1. *Diurnal cycle*

In the morning a surface based layer of statically stable air exists. Turbulence is generated in this layer due to the solar heating of the surface air. Convective wind slowly builds up developing a mixed boundary layer. These temporal variations in the thermal structure in the sodar echograms are being clearly seen in the records of Fig 3. The early morning acoustic sounder records on a nearly cloud free, clear, bright, windless sunny day can

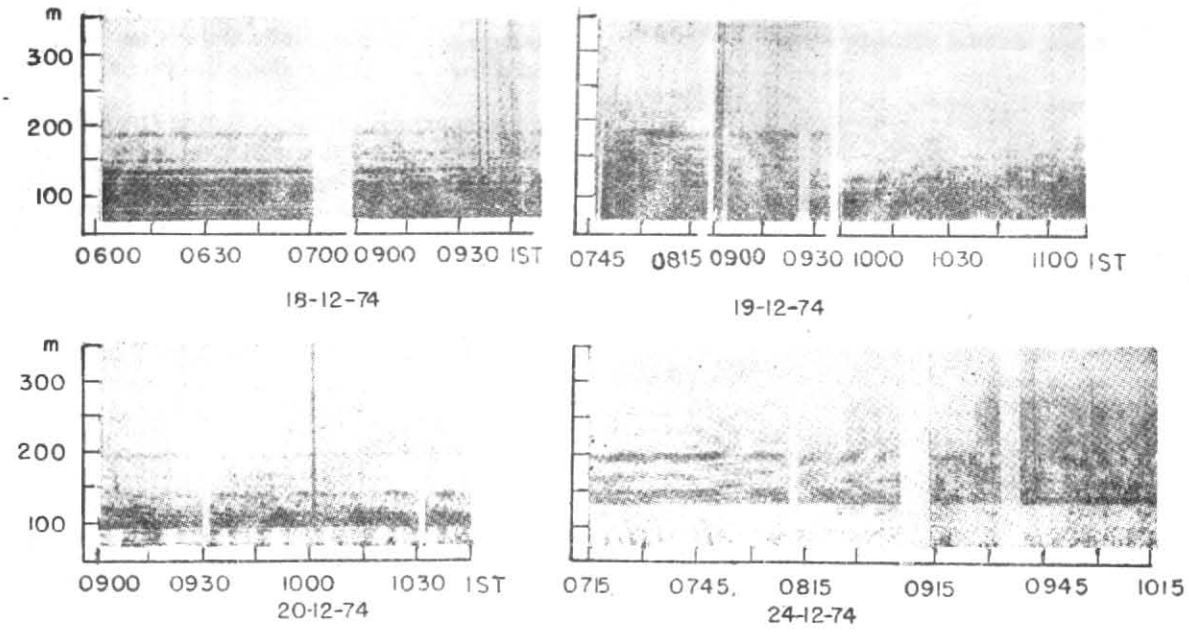


Fig. 3. Thermal structure during morning hours

thus detect the boundary of the mixed layer due to solar heating of the ground and the resulting temperature structure function $C_T$. A gradual increase in the mixing depth takes place as the solar heating of the surface progresses. At approximately 1200 IST solar heating becomes sufficiently intense and convective plumes (surface heated air parcels going up due to buoyancy) break through the inversion structure.

The convective activity continues in the afternoon until about 1600 hr in December and 1700 hr in April, when it starts subsiding and gets replaced by stable structure. The increasing uniformity of shading in the evening sounder return (Fig. 4) indicates the re-establishment of stable layer near the surface. The structure starts appearing in the form of growing thick layers which split up into stratified laminations as the radiative cooling of the ground and of the air in contact with it increases with time. The inversion layers are formed first very near the ground and later they extend to larger heights as the evening advances.

The night time echograms show multilayers (Fig. 5) superposed with undulations of a fairly wide range of frequency. The thickness of these layers varies from 10-50 metres depending on the weather conditions. The presence of these layers indicates turbulent regions within the otherwise thermally stable atmosphere. The typical height of these layers has been seen to be about 300 metres during December and about 200 metres during March-April. This height of the inversion structure is supported by the observed lapse rate measured by the radiosonde at Delhi (shown in the diagram as a plot of potential temperature and height).

### 3·2. *Wind shear*

Occasionally a strong elevated stable layer lasting for only a short time has been observed (Fig. 5 top echogram). This structure which has been mostly seen during extreme winter nights when the atmosphere is very stable, may be formed either due to the sudden appearance of a strong inversion layer at that level or due to a strong wind shear. The inversion formation is, however, a gradual phenomenon so the sudden appearance of a strong layer due to inversion is rather remote which leaves only the wind shear to give rise to a short lived strong elevated layer. This is further supported by the day time observations when a number of strong layers due to the surface winds are seen over-riding the plume structure.

### 3·3. *Stable waves*

On the night of 19-20 December 1974 an unusual feature in the stratified layer structure was seen (Fig. 5). There appeared a sinusoidal wave like turbulence which originated in the early hours of the night and lasted beyond mid-night. The amplitude of these waves reached a maximum at

about midnight after which it started subsiding. The wave motion was not continuous and had an average period of a few minutes. The sky on the night had been clear and the preceding day had been cloudless, bright and sunny.

The observed large amplitude wave motion has been found to be similar in structure to the stable waves (Bean *et al.* 1973 and Fengler and Stilke 1968—gravity waves or Kelvin-Helmholtz waves) which grow with time and gradually disappear because of internal forces within the wave. The wind shear in such cases may most often supply enough energy to set up wave motion with gravitation acting as a stabilizing or restoring force. The anomaly occurs within stable regions in zones of enhanced static stability with vertical shear of the horizontal wind accentuated (Richardson's number much less than 0·25). The period of such waves, as also in the present case, is generally within the range of 2-20 minutes depending on the specific stratification. These waves affect the electromagnetic field strength on their path because of the general correspondence of thermal conditions with humidity gradient, a behaviour also observed in the present case for the electromagnetic systems operating at the National Physical Laboratory.

The disturbance observed by the sodar on the night of 19-20 December 1974 was also clearly visible on the radiosonde observations. The initial refractivity gradient for the various days in and around the disturbance period (Fig. 7) shows the gradual steepening of the profile after 17 December 1974, peaking on 19-20 December and subsiding after 21 December. The initial refractivity gradient $\triangle N_i$ values reach a maximum value as high as 200 N/km (These values may, however, be still higher in actual practice since the first significant level for radiosonde observations refers to the 250 metres slab while the widths of the anomalous gradients are considerably narrower usually between 10-50 metres).

The actual meteorological origin of the disturbance of 19-20 December is not known but there is evidence to believe that it extended over a few hundered kilometres, a characteristic expected of stable waves.

### 3 .4. *Sodar indexing*

The structure on the sodar echogram as seen above is characteristic of the time, season and the ambient micrometeorological conditions of the lower atmosphere. These conditions determine the tropospheric propagation characteristics of the electromagnetic waves as also cause hazardous situations in aviation and air pollution. The characteristic information available from the sodar

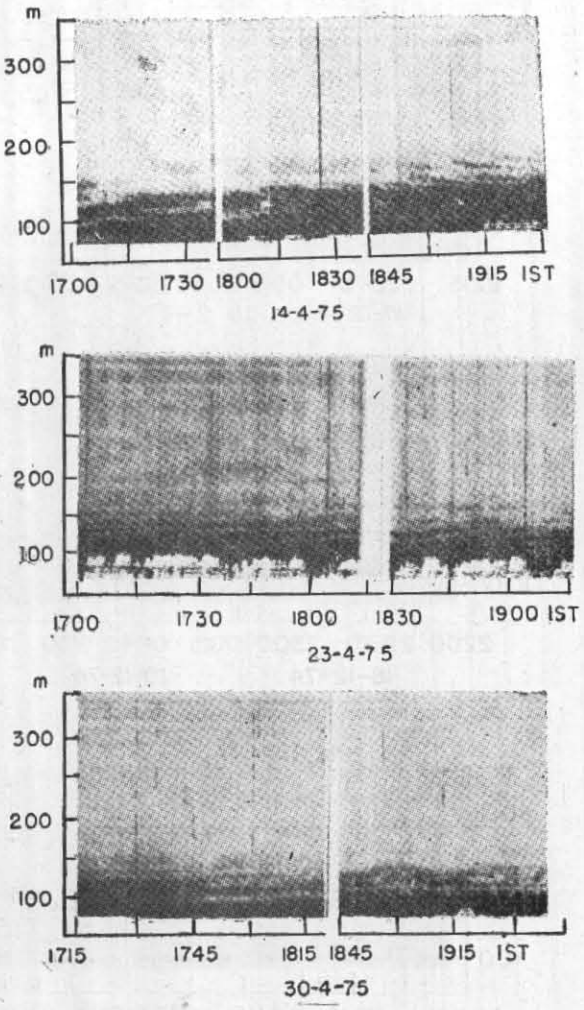


Fig. 4. Thermal structure during evening hours

echogram thus becomes an index for such situations. With this in view, the various types of observed structures on the sodar echograms have been indexed (Table 3 and Fig. 6). Starting from the zero index common to both day and night time structures, the day structures have been indexed separately from the night structures. The indexing has been done in both the cases in the increasing order of turbulence.

Zero index represents an atmosphere of weak temperature fluctuations with nearly adiabatic lapse rate. Under such conditions the scattered acoustic intensity is seen only in the lowest few tens of metres of the lower atmosphere.

During the day time the atmosphere is unstable due to solar heating. In the early morning the laminated inversion structure formed during the night breaks off. This transition structure is given the index number $ID_1$. This structure after more consistant heating of the ground surface develops into thermal plumes under clear, calm and sunny conditions. This is indexed as $ID_2$. The plume

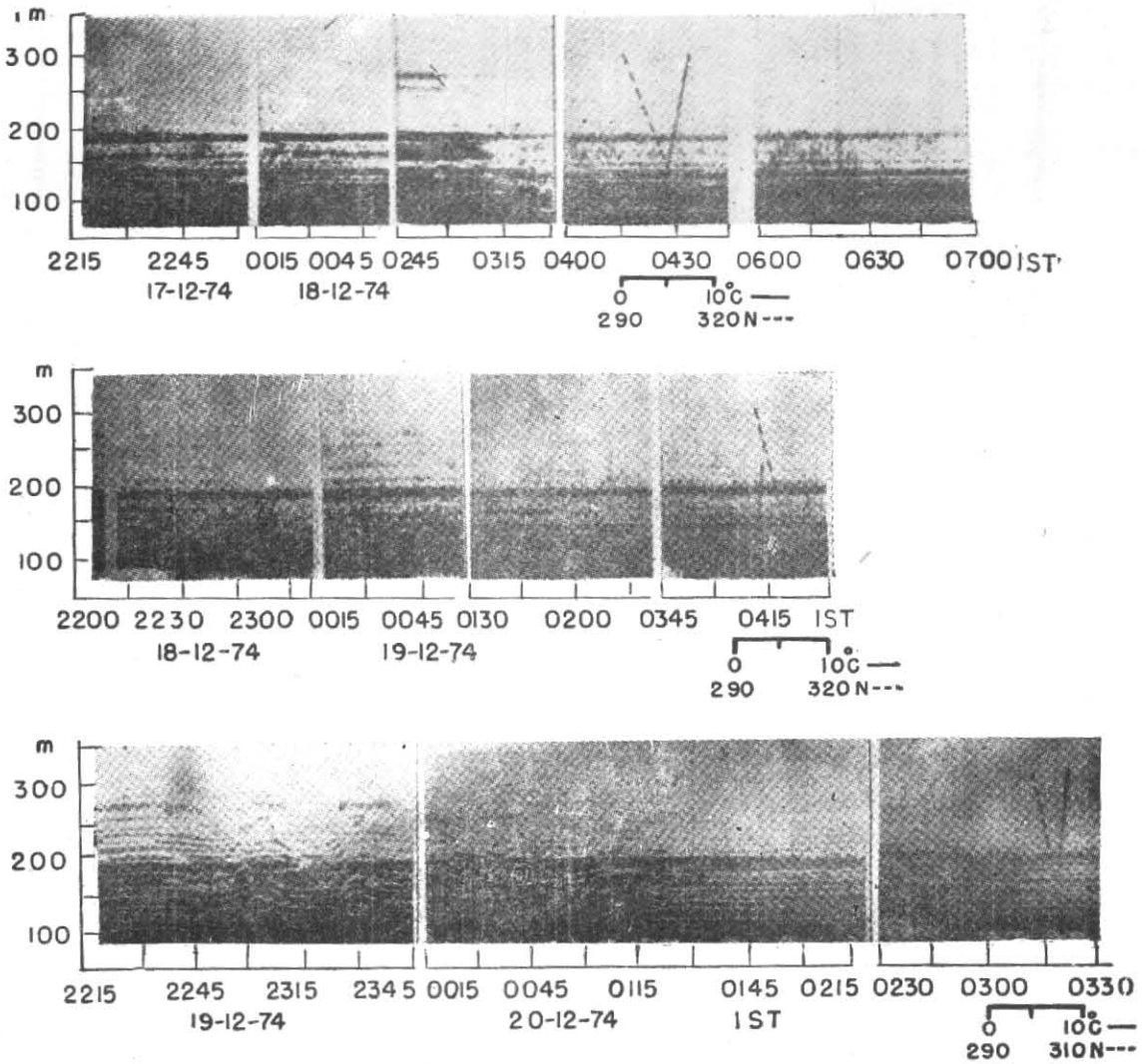


Fig. 5 (a). Thermal structure during night time

TABLE 2

Thermal data obtained with various Sodar Systems

| Period of operation | System operated collocated/ monostatic | Range of operation | | Resolution in height | Remarks |
|---|---|---|---|---|---|
| | | Minimum (range of ground clutter) (m) | Maximum (m) | (m) | |
| Jan 1972 to Mar 1972 | Collocated | 50 | 300 | 3 | Preliminary experiment using cross array and paraboloidal dish as antennas; recorded on photographic film |
| Jan 1974 to Apr 1974 | Collocated | 50 | 170 | 10 | Square array and reflector-horn used as transducers; recorder on facsimile reciever |
| Oct 1974 to Apr 1975 | Monostatic | 50 | 340 | 10 | Reflector horn used as transducer; recorded on facsimile receiver |
| Nov 1975 onwards | Monostatic | 50 | 600 | 100 | Reflector horn or paraboloidal bowl used as transducers; recorded on facsimile receiver |

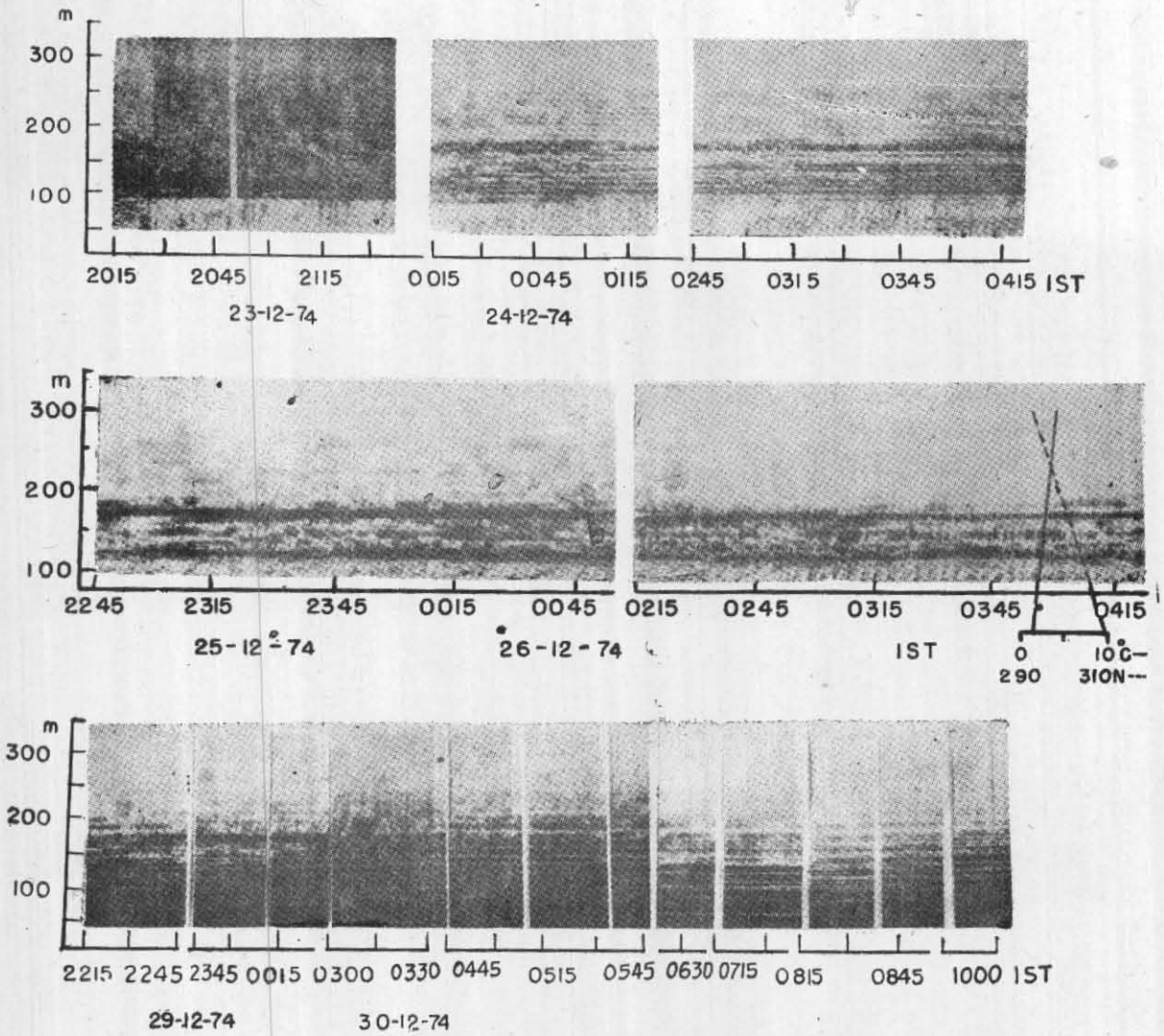


Fig. 5 (b). Thermal structure during night time in Dec 1974

**TABLE 3**

**Sodar indexing of atmospheric thermal structure**

Index Number Zero—No perceptible thermal structure, any time of the day, lapse rate zero, adiabatic conditions

| Index No. | Type of structure | Remarks | Index No. | Type of structure | Remarks |
|---|---|---|---|---|---|
| | *Sodar Indexing (Day time)* | | | *Sodar Indexing (Night time)* | |
| $ID_1$ | Breaking of layer structure and appearance of thermal plumes | Beginning of the unstable atmosphere | 1N | Formation of thick layers | Beginning of stable atmosphere |
| $ID_2$ | Formation of thermal plumes | Convective atmosphere, clear, bright, windless, sunny day | 2N | Stratified laminated layers with or without small undulations of wave periods | Radiation inversion, well settled stable atmosphere |
| 2D | Thermal plumes superposed with layers | Convective atmosphere mixed with surface winds | $3N_1$ | Appearance of a sudden additional short lived layer | Wind shear conditions |
| 3D | Persistent layer structure | Windless, cloudy day, no sun, stable conditions, persisting | $3N_2$ | The occurrence of plume like structure | Convective flow of winds |
| | | | 4N | Large amplitude wave motion superposed on laminated layer structure | Large instability generally encountered under stable conditions |

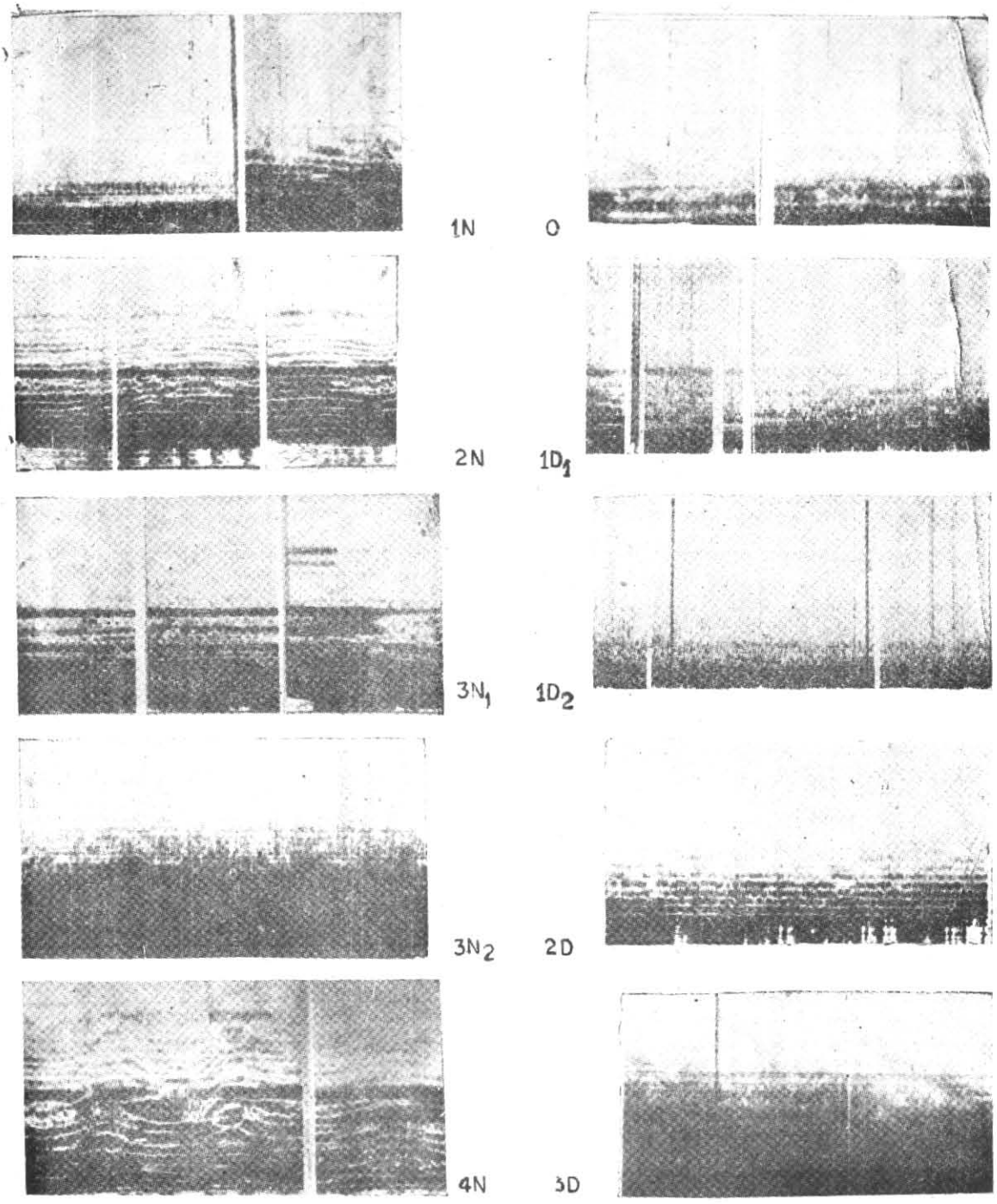


Fig. 6. Sodar atmospheric thermal structures (typical) and their indices

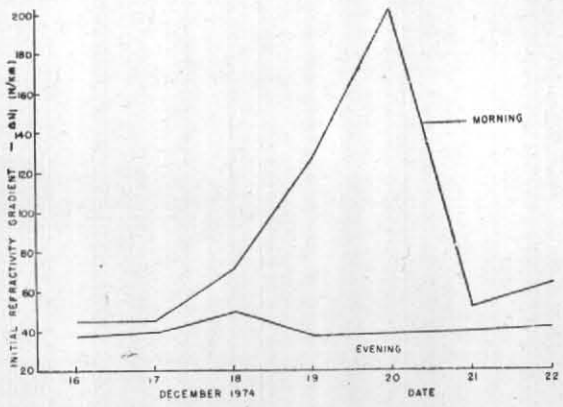


Fig. 7. The initial refractivity gradient plot for the various days in December 1974

structure gets superimposed with thick horizontal layers under conditions when light to medium surface winds blow during the day. The thickness of these layers and their number depends on the wind shear gradient. Such a structure is given the index number 2D. Sometimes, the clouds overcast the sky during the day and sun does not appear resulting in the absence of solar heating of the ground. Additionally there may be no mechanical disturbance. Under these conditions the nocturnal stratified layer structure can persist during the day also. This type of layering structure seen during the day is given the index number 3D.

During evening and night stable structure develops. Thick stable layers formed near the ground which grow in height developing more layers as evening advances, are given the index number 1N and represent strong stable conditions. Breaking up of these stable layers into stratified laminations during early night is given the index number 2N. Wind shear effects causing shifting of the laminated layers or appearance of a sudden additional layer for a short time at any level or the occurrence of plumes under stable conditions have been indexed as $3N_1$ and $3N_2$. Sometimes the stratified layer structure under stable conditions breaks up into a large sinusoidal wave like turbulence with a period of a few minutes. Such conditions are represented by index number 4N. The structure here represents a large instability encountered under stable conditions.

#### 4. Comparison of Sodar echogram intensities with radiosonde data

The extent to which the sodar echo intensity represents the radio refractivity conditions prevailing in the atmosphere can be studied by selecting a particular level on the sodar echogram, measuring its intensity level of blackness and comparing it with the refractivity gradient data as available from the radiosonde observations made simultaneously. This exercise has been done for the available sodar echograms at a height level of 150 metres. The measurements of the intensity of the received echo signal was made with the help of a microphotometer. The surface refractivity and the refractivity gradient numbers computed from the radiosonde observations at Delhi and the measured value of intensity for the sodar echograms are given in Tables 4 and 5. The prevailing ambient atmospheric conditions (also given) serve as a guide to compare the sodar echogram intensity with the refractivity gradient number.

It has been seen that only under clear and calm conditions, the two data can be compared. This is because sodar echograms are true representatives of the thermal structure of the lower atmosphere only under calm and clear weather conditions. These days are marked ($\surd$) on the diagrams. It is being seen that as the echo intensity increases, the refractivity gradient number becomes more negative. Echo intensities upto 10 dB correspond to a refractivity gradient number less than 40, echo intensities upto 25 dB correspond to a refractivity gradient number less than 70 and echo intensities higher than 25 dB correspond to a refractivity gradient number more than 70.

Radiosonde inversion predictions also correspond well with the echo intensities. Echo intensities less than 10 dB correspond to weak inversion, echo intensities less than 25 dB correspond to medium inversion and echo intensities more than 25 dB correspond to strong inversion.

#### 5. Thermal structure constant

Under unstable conditions, thermal structure parameter and temperature gradient are related as :

$$C_T = a\, S^{-2/3} \left(\frac{K_h}{K_m}\right)^{1/2} k^{2/3} Z^{-1/3} T^*$$

TABLE 4

**Comparison of Sodar echo intensity with refractivity gradient (height 150 m) — December 1974**

| Date (Dec 74) | Time (hr) | *Ns* | $\triangle N$/km negative | Echo intensity dB | Radiosonde inversion prediction | Remarks |
|---|---|---|---|---|---|---|
| 18 | 0430 | 320 | 69 | 21 | Medium | Foggy, no wind |
| | 1630 | 316 | 47 | 11 | Convective | Slight wind |
| 19 | 0430 | 319 | 135 | 32 | Strong | Foggy, no wind |
| | 1630 | 292 | 37 | 29 | Homogeneous | Winds |
| 20 | 1630 | 298 | 37 | 16 | Convective | Strong wind |
| 23 | 1630 | 295 | 46 | 13 | Convective | Clear, no wind |
| 24 | 0430 | 302 | 47 | 21 | Medium | Winds |
| | 1630 | 315 | 115 | 37 | — | No wind |
| 26 | 0430 | 304 | 55 | 19 | Strong | Slight wind |
| | 1630 | 299 | 90 | 21 | Medium | Cloudy, no wind |
| 27 | 1630 | 310 | 93 | 12 | Medium | Cloudy |
| 28 | 1630 | 306 | 67 | 5 | Convective | Cloudy |

TABLE 5

**Comparison of Sodar echo intensity with refractivity gradient (height 150 m) March-April 1975**

| Date (1975) | Time (hr) | *Ns* | $\triangle N$/km negative | Echo intensity dB | Radiosonde inversion prediction | Remarks |
|---|---|---|---|---|---|---|
| 26 Mar | 1645 | 286 | 26 | 9 | Weak | Clear, sunny, slight wind |
| 27 Mar | 0500 | 299 | 79 | 27 | Strong | Clear, no wind |
| 14 Apr | 1630 | 261 | 38 | 8 | Weak | Clear, sunny, slight wind |
| 15 Apr | 0430 | 285 | 33 | 19 | Medium | Clear, no wind |
| 18 Apr | 1630 | 278 | 38 | 9 | Weak | Cloud patches, slight wind |
| 23 Apr | 1700 | 308 | — | 8 | Homogeneous | Sunny, slight wind |
| 25 Apr | 0415 | 305 | — | 8 | Homogeneous | Clear, slight wind |
| 26 Apr | 1535 | 279 | — | 8 | Homogeneous | Sunny, slight wind |
| 29 Apr | 0445 | 299 | 119 | 11 | Strong | Clear, medium wind |
| 29 Apr | 1600 | 286 | — | 5 | Convective | Clear, windy |
| 30 Apr | 0430 | 293 | 53 | 12 | Strong | Clear, slight wind |
| 30 Apr | 1715 | 278 | 27 | 3 | Convective | Clear, sunny, no wind |
| 1 May | 0430 | 296 | 46 | 18 | Strong | Clear, no wind |

where $a$ is a constant estimated to be 0·47 from spectral measurements, $S$ is a non-dimensional wind shear term, $K_h$ and $K_m$ are the coefficients of heat conduction and viscosity respectively, $k$ is the von Karman's constant equal to 0·4, $Z$ is the vertical height and $T^*$ is the gradient of mean temperature $\frac{\partial \theta}{\partial (\log Z)}$. Tatarski (1961) extended the use of this theoretical relationship by calculating $C_T$ from independent meteorological measurements near the ground under both stable as well as unstable conditions and plotting them as a function of $k^{2/3} Z^{-1,3} T^*$. This plot gives a straight line behaviour under unstable conditions because '$S$' tends to be slighltly below one and

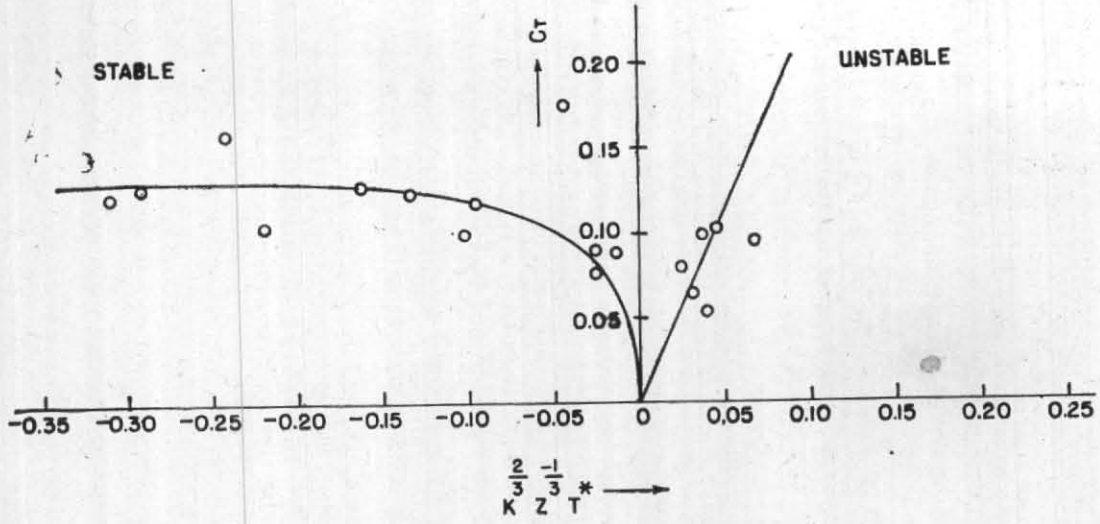


Fig. 8. Plot of sodar derived thermal structure constant $C_T$ as function of $k^{2/3} Z^{-1/3} T^*$

$K_h/K_m$ close to one under these conditions suggesting weak variations of $C_T$ with $S^{-2/3}$ $(K_h/K_m)^{1/2}$ while it shows a variable slope under stable conditions because $S$ under these conditions increases rapidly with increasing Richardson's number. This plot can thus be used as an index of the behaviour of the Richardson's number (turbulence parameter) as a function of thermal structure constant $C_T$.

Thermal structure parameter $C_T$ has been derived in the present experiments at a height of 150 metres from the received echo intensity on sodar echograms (For vertical sounding received power $P_r$ is proportional to $C_T^2/T^2$ with other parameters being experimental constants). The derived values of $C_T$ have been plotted as a function of $k^{2/3} Z^{-1/3} T^*$ (Fig. 8).The similarity in nature of the plot with that of Tatarski indicates that the intensity of the received signal on the sodar echograms can be used as an index of the variations in thermal structure parameter $C_T$ or in other words the turbulence parameter Richardson's number.

### 6. Conclusion

It is seen from the above studies that sodar echograms have a large potential in interpreting the micrometeorological conditions of the lower atmosphere continuously. The sodar indexing is very helpful for such situations as it can be used to convey this micrometeorological information just by a number. Sodar records can be used even to forecast hazardous situations before they actually occur. This can lead to the development of new forecasting techniques based solely on acoustic sounder records. The results as presented above are mostly qualitative. This is due to the lack of corresponding meteorological data. Attempts are being made to make these data available for comparison through the help of India Meteorological Department which is already in the process of development of slow rising readiosonde balloons. A sodar system has recently been set up at the Aya Nagar Observatory (Delhi) of the India Meteorological Department.

*Acknowledgements*

The authors are thankful to Dr. A. P. Mitra for the various suggestions made and guidance given during the course of the above work. We are thankful to the India Meteorological Department for loaning us the facsimile recorder and the radiosonde data. We are thankful to Mr. S. Parthasarthy of the National Physical Laboratory for loaning us the microphotometer facility. Lastly we are thankful to the photography section and the Workshop staff of the National Physical Laboratory for their time to time help.

*REFERENCES*


| | | |
|---|---|---|
| **Bean, B. R., Frisch, A. S., Mc Allister, L. G. and Pollard, J. R.** | 1973 | *Boundary layer meteorology*, **4**, p. 449. |
| **Fengler, G. and Stilke, G.** | 1968 | *Microwave propagation influenced by internal gravity waves*, AGARD Conference Proceedings, No. 37, Pt. I, 21-1 to 21-10. |
| **Kallistratova, M. A.** | 1961 | *Trudy Inst. Fiz. Atmos. Turbulentnost*, **4**, p. 203. |
| **Lumley, J. L. and Panofsky, H. A.** | 1964 | *The structure of atmospheric turbulence*, Inter Science Publishers, John Wiley and Sons, Inc., New York, p. 239. |
| **Monin, A. S.** | 1962 | *Sov. Phys. Acoust.*, **7**, p. 370. |
| **Singal, S. P. and Pancholy, M.** | 1972 | *J. Rad. and Space Phy.*, **1**, p. 202. |
| **Singal, S. P., Gera, B. S. and Aggarwal, S. K.** | 1975 (a) | *J. Pure and Applied Phys.*, **13**, p. 752. |
| **Singal, S. P., Gera, B. S., Aggarwal, S. K. and Mrs. Saxena, M.** | 1975 (b) | *Indian J. Radio and Space Phys.*, **4**, p. 146. |
| **Singal, S. P., Anand, J. R., Gera, B. S. and Aggarwal, S. K.** | 1975 (c) | *J. Rad. and Space Phys.*, **4**, p. 50. |
| **Tatarski, V. I.** | 1961 | *Wave propagation in a turbulent medium*, (Translator, R.A. Silverman), McGraw Hill Book Co. Inc., New York, Chapters 3 and 5. |